Cai, C., *et al.*: Numerical Analysis on the Transient Cavity Flow ...
THERMAL SCIENCE: Year 2019, Vol. 23, No. 3A, pp. 1387-1392

1387

NUMERICAL ANALYSIS ON THE TRANSIENT CAVITY FLOW FIELD DURING LIQUID NITROGEN JET FRACTURING

by

Chengzheng CAI[a,b], Keda REN[a,b], Shanjie SU[a,b], Menglin DU[a,b], and Zekai WANG[a,b]*

[a] State Key Laboratory for GeoMechanics and Deep Underground Engineering,
China University of Mining and Technology, China
[b] School of Mechanics and Civil Engineering, China University of Mining and Technology,
Xuzhou, China

Liquid nitrogen jet fracturing is expected to provide a novel treatment for reservoir stimulation. To verify its feasibility, the flow fields in cavity at different times are simulated by CFD method. Then the transient temperature and pressure distributions are analyzed. Based on the cavity pressure distributions, the pressure boosting effect is evaluated. The results show that the nitrogen gas close to the cavity entrance is easily pushed out and the temperature in this region decreases quickly during liquid nitrogen jet fracturing. However, the temperature at the cavity bottom increases firstly at the squeezing action of liquid nitrogen jet and then decreases due to the heat transfer induced by the low temperature liquid nitrogen jet. Compared with water jet, the liquid nitrogen jet can generate equivalent pressure boosting effect in the cavity. Due to the compressibility of nitrogen gas, the pressure boosting process of liquid nitrogen jet fracturing falls behind the hydrajet fracturing. This study identifies the pressure boosting capability of liquid nitrogen jet and can further provide theoretical basis for the researches of this fracturing treatment.

Key words: *fracturing, liquid nitrogen jet, pressure boosting, flow field,
numerical analysis*

Introduction

With the rapid progress of petroleum engineering, liquid nitrogen is expected to be an excellent substitution for water-based fracturing fluid [1]. As the liquid nitrogen is inert and anhydrous, the issues of reservoir damage and water excessive consumption can be effectively solved when it is used in well fracturing [2]. Under this background, a new fracturing treatment liquid nitrogen jet fracturing (LNJF) is proposed [3, 4]. For traditional hydrajet fracturing (HJF), the fracture initiation point can be controlled accurately just relying on the pressure boosting effect in the cavity [5]. Thus, for LNJF, the key of success fracturing is that whether the LNJ can also generate considerable pressure boosting effect.

Because of the great temperature difference between liquid nitrogen and formation fluid, the flow field in the cavity during LNJF will be more complex than HJF [6]. As the strong shear action of LNJ, the heat transfer phenomenon should be considered. In addition, the

---

change in liquid nitrogen physical properties probably influences the flow field in cavity, thereby playing a role in pressure boosting effect. Thus, it can be seen that the flow field in the cavity should be evaluated before the pressure boosting effect of LNJF is identified. In this paper, a 2-D CFD model for LNJF is built. Then the flow fields of LNJF at different times are analyzed.

The CFD model

The geometric model

A 2-D CFD model for the flow field during LNJF is built as shown in fig. 1. This model is composed of three parts: the nozzle region, the annulus region, and the cavity region. According to the experimental results of hydraulic perforating, the shape of the cavity is set as the spindle body [7]. Because of the symmetric structure of the model, only the half flow domain is
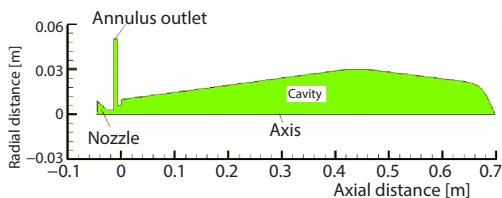

Figure 1. The geometric model for the flow field of LNJF

presented. The nozzle outlet diameter is 6 mm, the casing hole diameter is 14 mm, the annulus clearance is 15 mm. During the LNJF, the fluid enters into the flow domain through the nozzle, and then flows out through the annulus outlet. The nozzle inlet is set as pressure-inlet boundary, the annulus outlet is set as the pressure-outlet boundary, and the other walls are set as non-slip wall boundaries.

The governing equations

Due to the axisymmetric structure of the geometric model, the governing equation should be given in the cylindrical polar co-ordinate system. In this paper, the velocity, pressure and temperature distributions in the cavity at different times are simulated. Thus, the model involves unsteady flow and heat transfer. The physical properties of liquid nitrogen and nitrogen gas depend on the pressure and temperature. In this case, the governing equations consist of mass conservation, momentum conservation, energy conservation, turbulence and nitrogen property equations. The k-ε model is employed to simulate turbulent flow field and the NIST real gas models are adopted to calculate the density, isobaric heat capacity, viscosity, and thermal conductivity of nitrogen [8, 9]. The flow equations for 2-D axisymmetric geometries are given as [10]:

– mass conservation equation

$$\frac{\partial \rho}{\partial t} + \frac{\partial}{\partial x}(\rho v_x) + \frac{\partial}{\partial r}(\rho v_r) + \frac{\rho v_r}{r} = 0 \tag{1}$$

– momentum conservation equation

$$\frac{\partial(\rho v_x)}{\partial t} + \frac{1}{r}\frac{\partial}{\partial x}(r\rho v_x v_x) + \frac{1}{r}\frac{\partial}{\partial r}(r\rho v_r v_x) =$$

$$= -\frac{\partial p}{\partial r} + \frac{1}{r}\frac{\partial}{\partial x}\left[r\mu\left(2\frac{\partial v_x}{\partial x} - \frac{2}{3}(\nabla \vec{v})\right)\right] + \frac{1}{r}\frac{\partial}{\partial r}\left[r\mu\left(\frac{\partial v_x}{\partial r} + \frac{2}{3}\frac{\partial v_r}{\partial x}\right)\right] + F_x \tag{2}$$

$$\frac{\partial(\rho v_r)}{\partial t}\frac{1}{r}\frac{\partial}{\partial x}(r\rho v_x v_r) + \frac{1}{r}\frac{\partial}{\partial r}(r\rho v_r v_r) =$$

$$= -\frac{\partial p}{\partial r} + \frac{1}{r}\frac{\partial}{\partial x}\left[r\mu\left(\frac{\partial v_r}{\partial x} + \frac{\partial v_x}{\partial r}\right)\right] + \frac{1}{r}\frac{\partial}{\partial r}\left\{r\mu\left[2\frac{\partial v_r}{\partial r} - \frac{2}{3}(\nabla \vec{v})\right]\right\} - 2\mu\frac{v_r}{r^2} + \frac{2}{3}\frac{\mu}{r}(\nabla \vec{v}) + F_r \tag{3}$$

Cai, C., *et al.*: Numerical Analysis on the Transient Cavity Flow ...
THERMAL SCIENCE: Year 2019, Vol. 23, No. 3A, pp. 1387-1392

1389

– energy conservation equation

$$\frac{\partial(\rho T)}{\partial t} + \frac{\partial}{\partial x}(\rho v_x T) + \frac{\partial}{\partial r}(\rho v_r T) + \frac{\rho v_r T}{r} = \mathrm{div}\left(\frac{\lambda}{C_p}\,\mathrm{grad}\,T\right) + S_T \tag{4}$$

where ρ is the density, t – the time, x – the axial direction, r – the radial direction, v_x – the axial velocity, v_r – the radial velocity, $\vec{v}$ – the velocity vector, F_x and F_r are the components of the body forces, p – the pressure, T – the temperature, μ – the dynamic viscosity, C_p – the isobaric specific heat, and λ – the thermal conductivity.

Simulation results and analysis

In order to research the pressure boosting process during LNJF, a simulation case is conducted with the parameters as: inlet pressure, 45 MPa; outlet pressure, 20 MPa; injection temperature, 110 K; initial temperature, 330 K. In the beginning, the flow domain is assumed to be full of nitrogen gas. Meanwhile, the flow field of HJF is also simulated with the same inlet and outlet pressures. As the properties of water are insensitive to the pressure and temperature, the HJF is assumed to an isothermal flow and the energy equation is ignored. The physical parameters of water are set as: density, 998.2 kg/m³; viscosity, 10.03·10⁻⁴ Pa·s.

The temperature distributions

Unlike HJF, the LNJF involves heat transfer due to the great temperature difference between the LNJ and its surrounding fluid. Thus, the temperature distributions should be analyzed. Figure 2 shows the temperature contours of LNJF at different times. At 0.001 second, the LNJ just arrives at the cavity entrance and the temperature around the jet decreases obviously. As time passes by, the low temperature regions in annulus and cavity expand quickly. As shown in fig. 2, the annulus region has been full with liquid nitrogen since 0.1 second. This indicates that the high temperature nitrogen gas is pushed out due to the continuous injection of LNJ. However, from 0.1 second, the low temperature region in the cavity develops very slowly and the temperature of nitrogen gas at the cavity bottom presents an obvious increasing trend. It is because that due to the limited size of casing hole and the impact effect of LNJ, the nitrogen gas that is close to the cavity bottom is very difficult to be pushed out. On the contrary, the LNJ that enters into the cavity will generate the squeezing effect and do work on the nitrogen gas. Consequently, the temperature of nitrogen gas at cavity bottom increases.
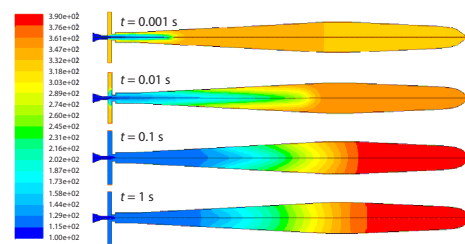

Figure 2. Temperature [K] contours of LNJF at different times
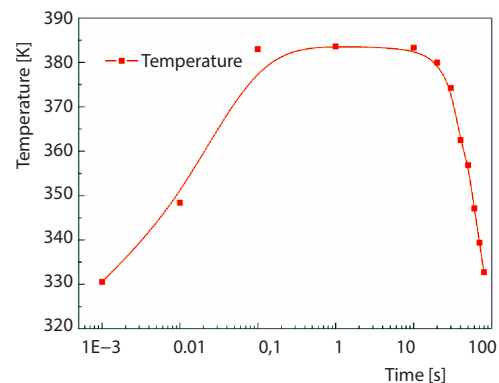

Figure 3. The temperatures in cavity terminus at different times

Figure 3 shows the temperatures of cavity terminus at different times. When the time is less than 1.0 second, the temperature of cavity terminus increases as time passes by. At 0.001

1390

Cai, C., *et al.*: Numerical Analysis on the Transient Cavity Flow ...
THERMAL SCIENCE: Year 2019, Vol. 23, No. 3A, pp. 1387-1392

second, the temperature of cavity terminus is 330.58 K, which is slightly higher than the initial value. As the time increases to 0.1 second, the temperature of cavity terminus is up to 382.97 K, presenting 15.85% higher than the initial value. This is because that the nitrogen gas in this region is compressed due to the squeezing effect of LNJ, which correspondingly leads to the temperature increasing. However, when the time is greater than 10 seconds, the temperature of cavity terminus begins to decrease with time. It is mainly because that the nitrogen gas becomes dense and difficult to be compressed. In this case, the heat transfer plays a domain role in the temperature change for the nitrogen gas close to the cavity terminus. Between 1.0 second and 10 seconds, the temperature of cavity terminus hardly changes. It indicates that during this period, the effects of LNJ squeezing and heat transfer on the temperature of cavity terminus are balanced.
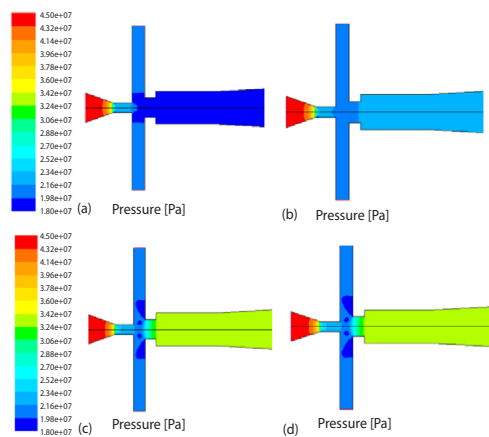

Figure 4. Pressure contours of LNJF at different times; (a) *t* = 0.001 s, (b) *t* = 0.01 s, (c) *t* = 0.1 s, and (d) *t* = 1 s
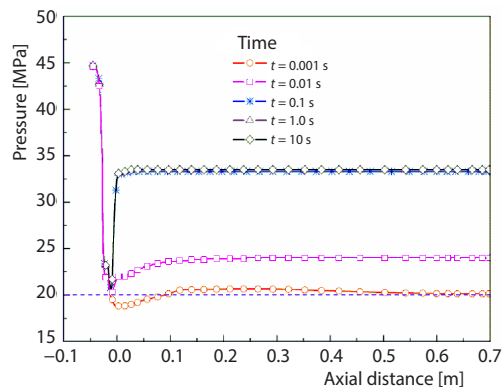

Figure 5. The pressure distributions along axial direction at different times during LNJF

The pressure distributions

As illustrated in fig. 4, the pressure of flow field change dramatically during LNJF. With the high pressure and low temperature liquid nitrogen continuously flowing into the flow domain, the pressure fields are redistributed. Along the axial direction, the pressure goes down firstly and then increases in the cavity. Finally, the pressure in the cavity is higher than the annulus and the pressure boosting effect is generated. As Qu *et al.* [5] indicates that due to the limited size of casing hole, the fluid that enters into the cavity within a short time cannot flows out immediately. In this case, the casing hole plays a similar sealing role during this process. From 0.1 second, the pressure in the cavity has become constant and the boost pressure, the pressure difference between the cavity and annulus, has reaches the maximum value.

To further research the pressure boosting effect in cavit y during LNJF, the pressure distributions along axial direction at different times are analyzed. As shown in fig. 5, the pressure in cavity is roughly equal to the initial value at 0.001 seconds. This indicates that the pressure boosting effect has not been produced yet. In contrast, the pressure near the entrance of cavity decreases by 1.21 MPa. It is because that as the LNJ just arrives at the cavity, the kinetic energy that is carried by jet is very limited. Thus, the LNJ is insufficient to generate the pressure boosting effect. Additionally, the low temperature LNJ can cause the ambient temperature decreasing, which induces the reduction of fluid volume. As a result, the pressure near the cavity entrance also decreases. With the continuous injection of LNJ, the pressure in cavity begins to increase. At 0.01 second, the pressure in cavity

Cai, C., *et al.*: Numerical Analysis on the Transient Cavity Flow ...
THERMAL SCIENCE: Year 2019, Vol. 23, No. 3A, pp. 1387-1392

1391

is up to 24.04 MPa. At 0.1 second, this value has increased to 33.30 MPa, indicating a boost pressure of 13.30 MPa. After 1.0 second, the pressure in cavity keeps at 33.50 MPa, only 0.20 MPa higher than that at 0.01 second. This indicates that the effective pressure boosting effect of LNJF has been produced since 0.01 second.

To evaluate pressure boosting ability of LNJF, the cavity pressures of LNJF and HJF at different times are compared. As shown in fig. 6, when the cavity pressure becomes steady, the boost pressure of LNJF is slightly higher than HJF. This indicates that the LNJF can also perform excellent pressure boosting effect like HJF. In addition, the pressure boosting process

Figure 6. The pressures in cavity of LNJF and HJF at different times

of LNJF is more slowly than the HJF. For example, the pressure boosting of HJF almost finishes at 0.001 second while the LNJF performs effective pressure boosting effect at 0.1 second. Thus, the fracture initiation of LNJF is probably later than HJF for field application.
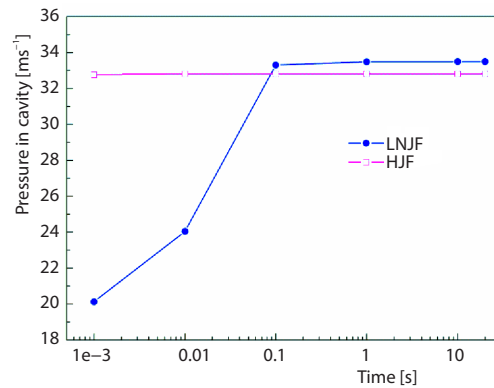
Conclusion

In our work, a 2-D CFD model is built to simulate the flow field for LNJF. Using this model, the temperature and pressure distributions are researched. The results show that as the low temperature LNJ arrives at the cavity, the temperature near the cavity entrance decreases quickly. However, the temperature at the cavity bottom increases firstly and then decreases as time passes by. This is because that at initial stage, the nitrogen gas at the cavity bottom is compressed by the LNJ. As the nitrogen gas is hard to be compressed, the heat transfer will play a domain role in temperature change. Compared with HJF, the LNJF also presents enough pressure boosting performance in the cavity. However, the rate of pressure boosting is smaller than HJF. This work reveals the flow field and evaluates the pressure boosting effect of LNJF.

Acknowledgment

Nomenclature

C_p – isobaric heat capacity, [Jkg^{-1}K^{-1}]
F_x, F_r – components of body forces, [kgm^{-1}s^{-1}]
p – pressure, [Pa]
r, x – radial and axial directions, [m]
S_T – term for viscous dissipation, [Ks^{2}m^{-2}]
T – temperature, [K]
t – time, [s]

$\vec{v}$ – velocity vector, [ms^{-1}]
v_x, v_r – axial and radial velocities, [ms^{-1}]

Greek symbols

λ – thermal conductivity, [Wm^{-1}K^{-1}]
μ – viscosity of nitrogen, [Pa·s]
ρ – density, [kgm^{-3}]

References

[1] Wang, L., *et al.,* Waterless Fracturing Technologies for Unconventional Reservoirs-Opportunities for Liquid Nitrogen, *Journal of Natural Gas Science and Engineering*, *35* (2016), Part A, pp. 160-174
[2] Cai, C., *et al*., The Effect of Liquid Nitrogen Cooling on Coal Cracking and Mechanical Properties, *Energy Exploration & Exploitation*, *36* (2018), 6, pp. 1609-1628
[3] Zhang, S., *et al*., Numerical and Experimental Analysis of Hot Dry Rock Fracturing Stimulation with

1392

Cai, C., *et al.*: Numerical Analysis on the Transient Cavity Flow ...
THERMAL SCIENCE: Year 2019, Vol. 23, No. 3A, pp. 1387-1392

High-Pressure Abrasive Liquid Nitrogen Jet, *Journal of Petroleum Science and Engineering*, *163* (2018), Apr., pp. 156-165

[4] Cai, C., *et al*., Feasibility of Reservoir Fracturing Stimulation with Liquid Nitrogen Jet, Journal of Petro-*leum Science and Engineering*, *144* (2016), Aug., pp. 59-65

[5] Qu, H., *et al*., The Boosting Mechanism and Effects in Cavity during Hydrajet Fracturing Process, *Petro-leum Science and Technology*, *28* (2010), 13, pp. 1345-1350

[6] Cai, C., *et al*., Downhole Transient Flow Field and Heat Transfer Characteristics during Drilling with Liquid Nitrogen Jet, *Journal of Energy Resources Technology – Transactions of the ASME*, *140* (2018), 12, pp. 122902

[7] Cheng, Y., *et al.*, Flow Field Character in Cavity during Supercritical Carbon Dioxide Jet Fracturing (in Chinese), *Journal of China University of Petroleum (Edition of Natural Science), 38* (2014), 4, pp. 81-86

[8] Span, R., *et al*., A Reference Equation of State for the Thermodynamic Properties of Nitrogen for Tem-peratures from 63.151 K to 1000 K and pressures to 2200 MPa, *Journal of Physical and Chemical Refer-ence Data*, *29* (2000), 6, pp. 1361-1433

[9] Lemmon, E. W., Jacobsen, R. T., Viscosity and Thermal Conductivity Equations for Nitrogen, Oxygen, Argon, and Air, *International Journal of Thermophysics*, *25* (2004), 1, pp. 21-69

[10] Batchelor, G. K., *An Introduction Fluid Dynamics*, Cambridge University Press, Cambridge, UK, 2000